

Simulation of traffic flow at a signalised intersection

M. Ebrahim Foulaadvand *

*Department of Nano-Science, Institute for Studies in Theoretical Physics and Mathematics (IPM),
P.O. Box 19395- 5531, Tehran, Iran and Department of Physics,
Zanjan University, P.O. Box 45195-313, Zanjan, Iran.*

Sommayeh Belbaasi

Department of Physics, Zanjan University, P.O. Box 45195-313, Zanjan, Iran.

(Dated: September 3, 2018)

We have developed a Nagel-Schreckenberg cellular automata model for describing of vehicular traffic flow at a single intersection. A set of traffic lights operating either in fixed-time or traffic adaptive scheme controls the traffic flow. Closed boundary condition is applied to the streets each of which conduct a uni-directional flow. Extensive Monte Carlo simulations are carried out to find the model characteristics. In particular, we investigate the dependence of the flows on the signalisation parameters.

I. INTRODUCTION

Modelling the dynamics of vehicular traffic flow by cellular automata has constituted the subject of intensive research by statistical physics during the past years [1, 2, 3, 4]. *City traffic* was an early simulation target for statistical physicists [5, 6, 7, 8, 9, 10, 11, 12, 13, 14, 15]. Evidently the optimisation of traffic flow at a single intersection is a preliminary but crucial step to achieve the ultimate task of global optimisation in city networks [16]. Nagatani proposed the first model for simulation of two crossing streets [17]. Subsequently, Ishibashi and Fukui developed similar models [18, 19]. Recently, physicists have notably attempted to simulate the traffic flow at intersections and other traffic designations such as roundabouts [20, 21, 22, 23, 24, 25, 26, 27, 28, 29, 30, 31, 32, 33]. In principle, the vehicular flow at the intersection of two roads can be controlled via two distinctive schemes. In the first scheme, the traffic is controlled without traffic lights [33, 34]. In the second scheme, signalised traffic lights control the flow. In Ref.[22], we have modelled the traffic flow at a single intersection with open boundary conditions on streets. Dependence of waiting times on signalisation and inflow rates were investigated in details. Along this line of study, our objective in this paper is to study in some depth, the characteristics of traffic flow and its optimisation in a single intersection with closed boundary condition. We will compare our results to those obtained in our recent study of a nonsignalised intersection [33]. In order to capture the basic features of this problem, we have constructed a NS cellular automata model. This paper has the following layout. In section II, the model is introduced and formulated. In sections III and IV, the results of Monte Carlo simulations of each controlling scheme are exhibited. Concluding remarks and discussions ends the paper in section V.

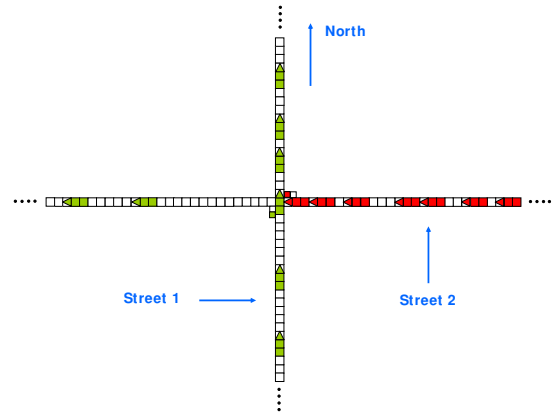


FIG. 1: Intersection of two uni-directional streets.

II. DESCRIPTION OF THE PROBLEM

Imagine two perpendicular one dimensional closed chains each having L sites. The chains represent urban roads accommodating unidirectional vehicular traffic flows. They intersect each other at the middle sites $i_1 = i_2 = \frac{L}{2}$ on the first and the second chain. With no loss of generality we take the flow direction in the first chain from south to north and in the second chain from east to west. (see Fig.1 for illustration). Cars are not allowed to turn. The discretisation of space is such that each car occupies an integer number of cells denoted by L_{car} . The car position is denoted by the location of its head cell. Time elapses in discrete steps of Δt and velocities take discrete values $0, 1, 2, \dots, v_{max}$ in which v_{max} is the maximum velocity.

To be more specific, at each step of time, the system is characterized by the position and velocity configurations of cars. The system evolves under the Nagel-Schreckenberg (NS) dynamics [35]. Let us now specify the physical values of our time and space units. The length of each car is taken 4.5 metres. Therefore, the spatial grid Δx (cell length) equals to $\frac{4.5}{L_{car}}$ m. We take

*Corresponding author: foolad@iasbs.ac.ir

the time step $\Delta t = 1$ s. Furthermore, we adopt a speed-limit of 75 km/h. The value of v_{max} is so chosen to give the speed-limit value 75 km/h or equivalently 21 m/s. In this regard, v_{max} is given by the integer part of $21 \times L_{car}/4.5$. For instance, for $L_{car} = 5$, v_{max} equals 23. In addition, each discrete increments of velocity signifies a value of $\Delta v = \frac{4.5}{L_{car}} m/s$ which is also equivalent to the acceleration. For $L_{car} = 5$ this gives the comfort acceleration $0.9 \frac{m}{s^2}$. Moreover, we take the value of random breaking parameter at $p = 0.1$. A set of traffic lights controls the traffic flow. We discuss two types of signalisation in this paper: *fixed-time* and *traffic responsive*.

III. FIXED TIME SIGNALISATION OF LIGHTS

In this scheme the lights periodically turn into red and green. The period T , hereafter referred to as *cycle time*, is divided into two phases. In the first phase with duration T_g , the lights are green for the northward street and red for the westward one. In the second phase which lasts for $T - T_g$ timesteps the lights change their colour i.e.; they become red for the northward and green for the westward street. The gap of all cars are update with their leader vehicle except those two which are the nearest approaching cars to the intersection. These two cars need special attention. For these approaching cars gap should be adjusted with the signal in its red phase. In this case, the gap is defined as the number of cells right after the car's head to the intersection point $\frac{L}{2}$. If the head position of the approaching car lies in the crossing point the gap is zero. We note that at the time step when the traffic light goes red for a direction, portion of a car from that direction can occupy the crossing point. In this case the leading car of the queue in the other direction should wait until the passing car from the crossing point completely passes the intersection i.e.; its tail cell position become larger than $\frac{L}{2}$. Now all the computational ingredients for simulation is at our disposal. The streets sizes are $L_1 = L_2 = 1350$ m and we take $L_{car} = 5$. The system is update for 2×10^5 time steps. After transients, two streets maintain steady-state currents denoted by J_1 and J_2 which are defined as the number of vehicles passing from a fixed location per time step. They are functions of global densities ρ_1 and ρ_2 and signal times T and T_g . We kept ρ_2 fixed in the second street and varied ρ_1 . Figure (2) exhibits the fundamental diagram of the first street i.e.; J_1 versus ρ_1 . The parameters are specified in the caption.

We observe that for each T_g , J_1 linearly increase up to $\rho_1 = \rho_-$, then a lengthy plateau region is formed up to $\rho_1 = \rho_+$. If T_g increases, ρ_- becomes larger, ρ_+ becomes smaller, and the plateau height increases. This seems natural because by increasing T_g the model tends to a normal NS model. The emergence of a plateau region is associated to defect-like role of the crossing point. The asymmetric simple exclusion process (ASEP), as a paradigm for non equilibrium processes in one dimension,

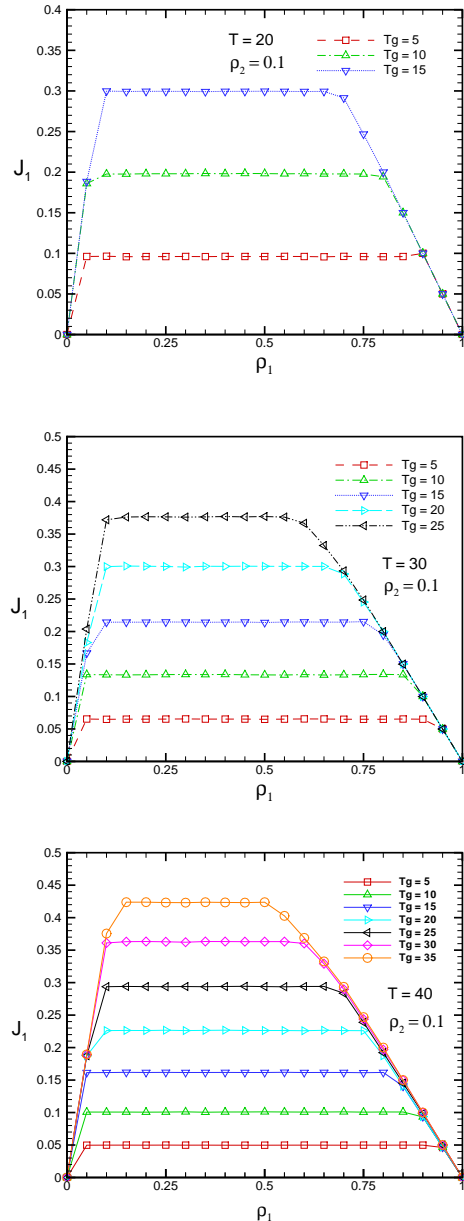


FIG. 2: J_1 vs ρ_1 for various values of T_g at fixed $\rho_2 = 0.1$. $T = 20$ (top), $T = 30$ (middle) and $T = 40$ (bottom).

with one defective site has been investigated within the Bethe Ansatz formalism in [36] and matrix product state [37]. It is a well-established fact that a local defect can affect the low dimensional non-equilibrium systems on a global scale. This has been confirmed not only for ASEP [34, 38, 39, 40] but also for cellular automata models describing vehicular traffic flow [41, 42]. After the plateau, J_1 exhibits linear decrease versus ρ_1 in the same manner as in the fundamental diagram of a single road. Concerning the variation of cycle time T , increasing the cycle time T gives rise, on an equal basis, to increase both in

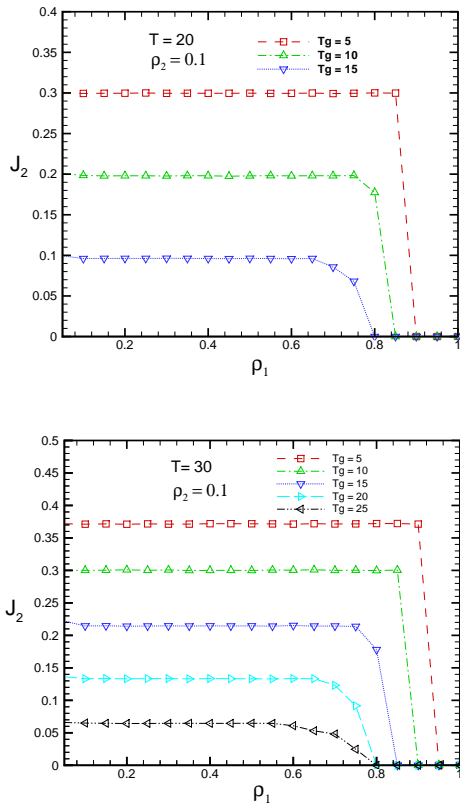


FIG. 3: J_2 vs ρ_1 for various T_g at $\rho_2 = 0.1$. Top: $T=20$ and bottom: $T=30$.

the green and in the red portion of the cycle allocated to each street. The results show a notable increase in flows when T is increased. This observation does not seem to comply to reality. The reason is due to unrealistic nature of NS rules. We now consider the flow properties in the second street. In Figure (3) we depict the behaviour of J_2 versus ρ_1 for various values of T_g .

Although ρ_2 remains constant J_2 is affected by density variations in street 1. For each T_g , J_2 as a function of ρ_1 exhibits two regimes. In the first regime, J_2 is almost independent of ρ_1 and remains constant up to ρ_+ . Afterwards in the second regime, J_2 exhibits a linearly decreasing behaviour towards zero. Analogous to J_1 , the existence of a wide plateau region indicates that street 2 can maintain a constant flow capacity for a wide range of density variations in the first street. If T_g is increased, the green time allocated to the second street decrease so we expect J_2 to exhibit a diminishing behaviour. This is in accordance to what figure (3) shows. In order to find a deeper insight, it would be illustrative to look at the behaviour of total current $J_{tot} = J_1 + J_2$ as a function of density in one of the streets. Evidently for optimisation of traffic one should maximize the total current J_{tot} therefore it is worth investigating how the total current behaves upon variation of the model parameters. Fig.(4) sketches this behaviour.

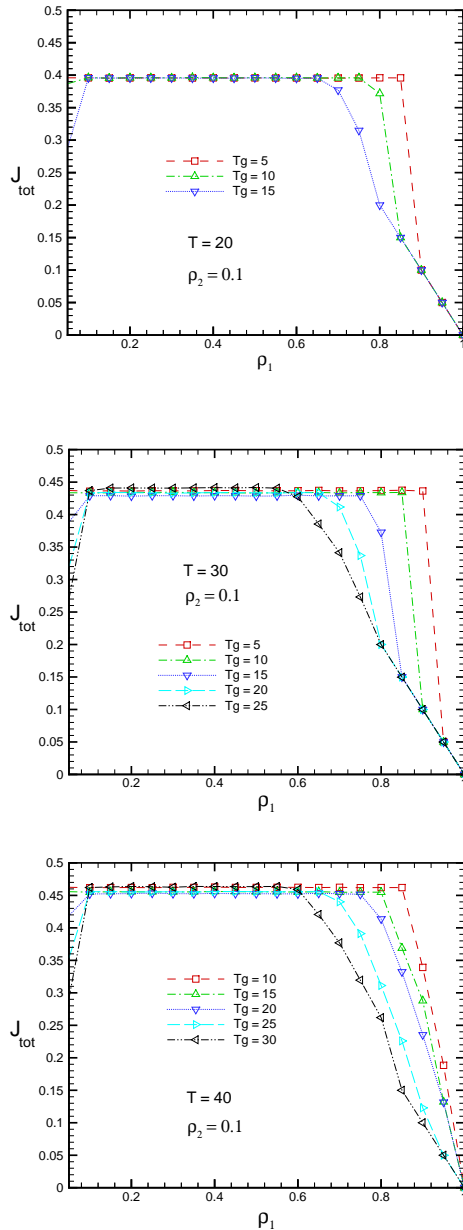


FIG. 4: J_{tot} vs ρ_1 for various values of T_g at $\rho_2 = 0.1$: $T = 20$ (Top), $T = 30$ (middle) and $T = 40$ (bottom).

In general, the dependence of total current on J_1 depends on the value of T_g . Except for small values of T_g , total current increases with ρ_1 then it becomes saturated at a lengthy plateau before it starts its linear decrease. We have also examined the behaviour of J_{tot} for other values of ρ_2 . Figures (5) exhibits the results for $\rho_2 = 0.05$ and $\rho_2 = 0.5$ respectively.

Our simulations confirm that for small ρ_2 up to 0.1 total current shows a distinguishable dependence on T_g in the entire range of ρ_1 especially in intermediate values. In contrast, for $\rho_2 > 0.1$, we observe no significant

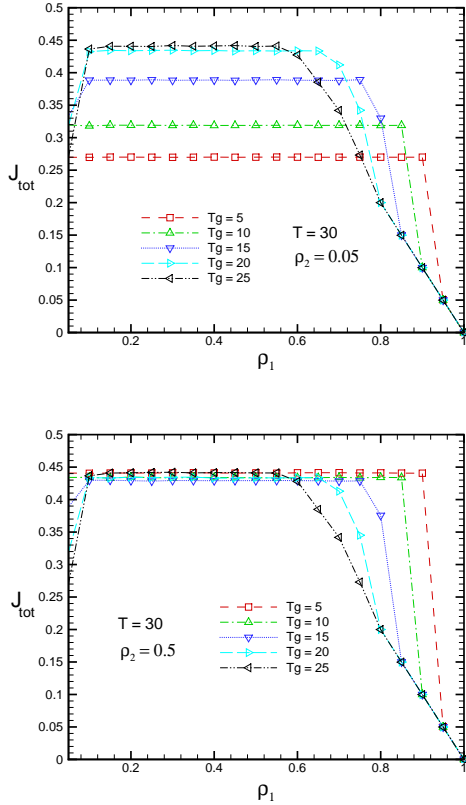


FIG. 5: Total current J_{tot} vs ρ_1 for various values of T_g at $T = 30$: $\rho = 0.05$ (Top) and $\rho = 0.5$ (bottom).

dependence on T_g in the intermediate ρ_1 but we observe notable dependence for large ρ_1 .

A. Density profile and Queue Formation

In this section we try to investigate, in brief, the characteristics of queues which are formed behind the crossing point in the course of the red periods. To this end, in the following set of figures we exhibit the profile of density in the vicinity of intersection. This will provide much insight into the problem. In figure (6) we have sketched such profiles for three values of green times T_g .

At each global density ρ_1 a high density region, hereafter referred to as HD, forms behind the crossing point. This corresponds to queue formation behind the crossing point. The length and height of this HD region grows with ρ_1 . Keeping ρ_1 constant, the length as well as the height of the HD region decreases with increasing T_g . This is expected since by increasing T_g the cars in the first street are given more time to pass the intersection and less cars will have to stop at red periods. Right after the crossing point, we observe a quick relaxation of the density profile to a low density region (hereafter referred to as LD). It would be natural to interpret the length

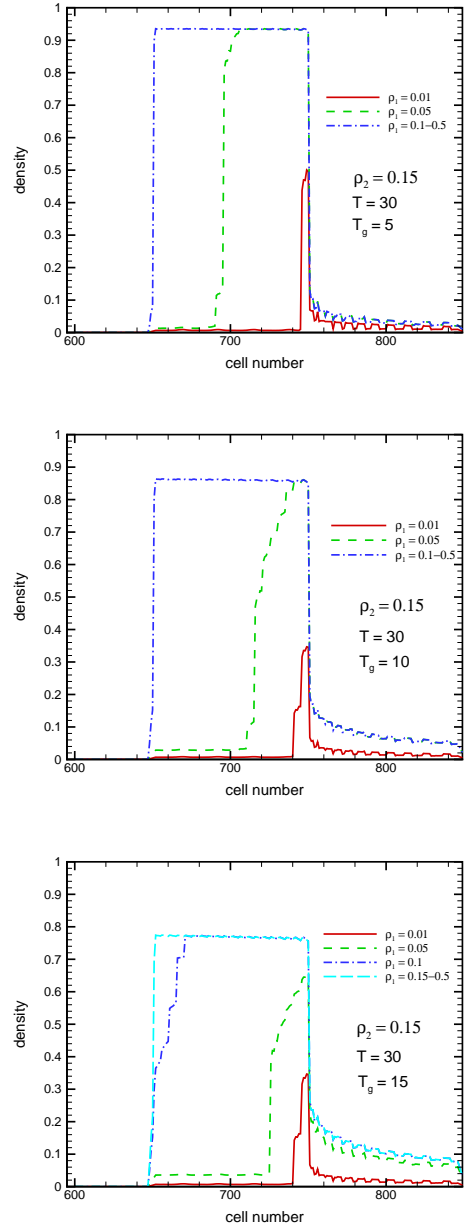


FIG. 6: Density profile of the first street for given values of parameters which are specified in the figures. Crossing site is at 750th cell.

of the HD region as the average queue length. We note that small oscillation in the profiles are not associated to inadequacy of simulation time. In fact their emergence is related to the updating rules of the NS model. Such oscillations have also been observed in the density-density correlation function in the NS model [43].

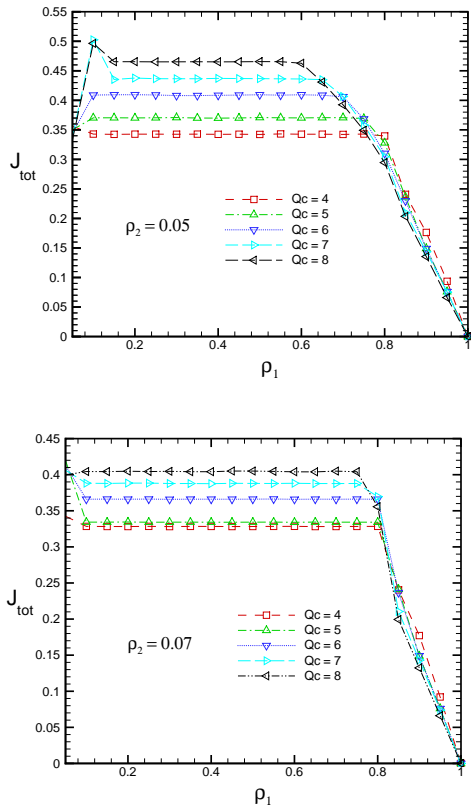


FIG. 7: Total current vs ρ_1 at $\rho_2 = 0.05$ (top) and $\rho_2 = 0.07$ (bottom) for various values of Q_c .

IV. TRAFFIC RESPONSIVE SIGNALISATION

In this section we present our simulation results for the *so-called* intelligent controlling scheme in which the traffic light cycle is no longer fixed [44, 45]. In this scheme which is sometimes called *traffic responsive*, the signalisation of traffic lights is simultaneously adapted to traffic status in the vicinity of intersection. This scheme has been implemented in simulation of traffic flow at intersections with open-boundary conditions [22, 24]. There exist numerous schemes in which traffic responsive signalisation can be prescribed. Three of these schemes are discussed in [22]. Here for brevity we discuss only one of these methods. To be precise, we define a cut-off queue length Q_c . The signal remains red for a street until the length of the corresponding queue formed behind the red light exceeds the cut-off length Q_c . At this moment the lights change colour. Apparently due to stochastic nature of cars movement, the cycle time will be subjected to variations and will no longer remain constant. In figure (7) we exhibit J_{tot} versus ρ_1 for various values of cut-off lengths Q_c and ρ_2 .

Analogous to fixed-time scheme, for given ρ_2 a lengthy plateau in J_{tot} forms. The plateau height as well as its length show a significant dependence on Q_c . Higher Q_c

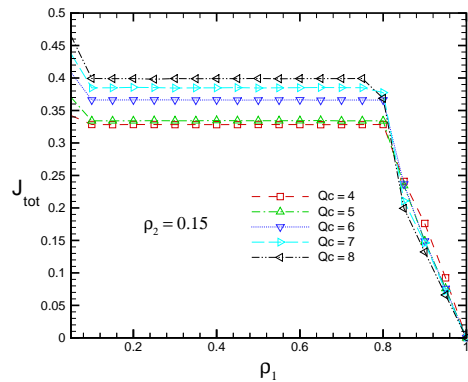


FIG. 8: J_{tot} vs ρ_1 at $\rho_2 = 0.15$ for various values of Q_c .

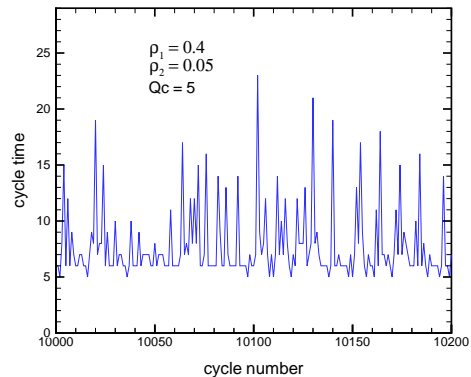


FIG. 9: Variation of cycle lengths in traffic responsive scheme for 200 cycles.

are associated with smaller length and higher current. We have also examined larger values of ρ_2 . The results are qualitatively analogous to the above graphs. The notable point is that for ρ_2 larger than 0.1, J_{tot} does not show a significant dependence on ρ_2 . Figure (8) depicts J_{tot} versus ρ_1 for $\rho_2 = 0.15$.

In figure (9) we have depicted the cycle lengths in the traffic responsive scheme which vary from cycle to cycle. The appearance of such behaviour remarks the adaptation of traffic lights in the responsive scheme.

To shed some light on the problem, we sketch space-time plots of vehicles. It is seen that in traffic responsive scheme, the cars spatial distribution is more homogeneous which is due to randomness in cycle times.

Lastly, we compare our results to those obtained in simulation of a nonsignalised intersection [33]. In a nonsignalised intersection, the cars yield to each other upon approaching the crossing point and the priority is given to the car which is closer to the crossing point. The total current versus ρ_1 in a nonsignalised intersection has the following form:

For ρ_2 larger than 0.1, the optimal current is roughly

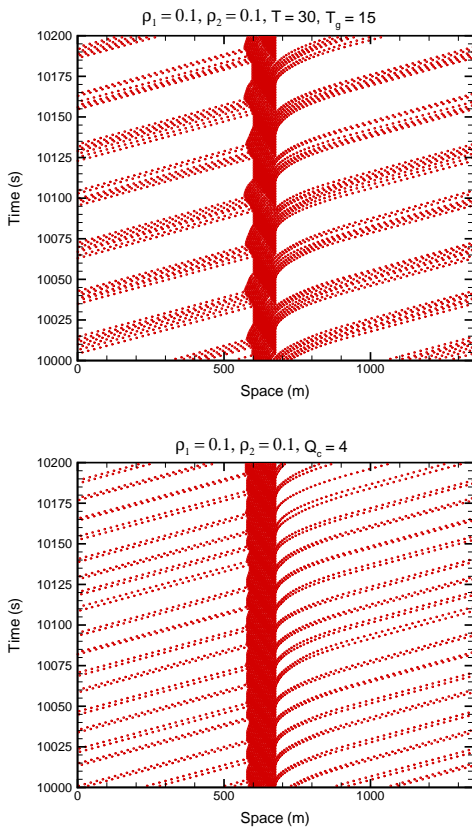


FIG. 10: Space-time plot of vehicles for fixed time (top) and traffic responsive schemes (bottom).

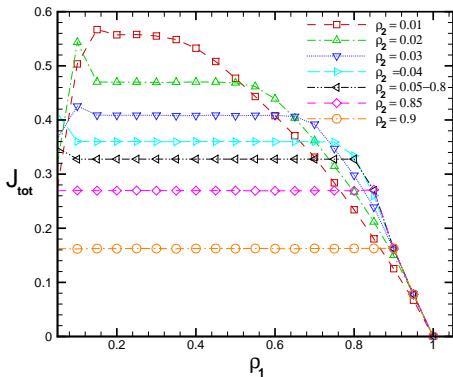


FIG. 11: J_{tot} vs ρ_1 for various values of ρ_2 in a nonsignalised intersection.

0.33 in the nonsignalisation scheme whereas in the signalised scheme with a fixed time strategy, the optimal value of J_{tot} reaches beyond 0.45 (see Figs. 4 and 5) in a fixed time scheme and 0.4 in the traffic responsive scheme. It can be concluded that signalisation strategies are apparently more efficient in comparison to non-signalisation scheme.

V. SUMMARY AND CONCLUDING REMARKS

By extensive Monte Carlo simulations, we have investigated the flow characteristics in a signalised intersection via developing a Nagel-Schreckenberg cellular automata model. We have considered two types of schemes: fixed-time and traffic responsive. In particular, we have obtained the fundamental diagrams in both streets and the dependence of total current on street densities. Our findings show hindrance of cars upon reaching the red light gives rise to formation of plateau regions in the fundamental diagrams. This is reminiscent of the conventional role of a single impurity in the one dimensional out of equilibrium systems. The existence of wide plateau region in the total system current shows the robustness of the controlling scheme to the density fluctuations. The overall throughput from the intersection shows a significant dependence on the cycle time in the fixed time scheme and on the queue cut-off length in the responsive scheme. Moreover, by plotting the density profiles, we have been able to quantify the characteristics of queues. Comparison to our previous results for a nonsignalised intersection shows the higher efficiency of the signalisation strategy. We remark that our approach is open to serious challenges. The lack of empirical data prevents us to judge how much our results are close to and to what degree they differ from reality. Our CA model allows for varying space and time grids. By their appropriate adjusting, we are able to reproduce a realistic acceleration. We emphasize that our model suffers from non realistic behaviour of car movement when the lights turn green. The crucial point is to model the braking and accelerating as realistic as possible. Empirical data are certainly required for this purpose. We expect the system characteristics undergo substantial changes if realistic yielding declaration is taken into account.

VI. ACKNOWLEDGEMENT

We highly appreciate M. Abol Bashar for his fruitful helps and enlightening discussions.

[1] D. Chowdhury, L. Santen and A. Schadschneider, *Physics Reports*, **329**, 199 (2000).
 [2] D. Helbing, *Rev. Mod. Phys.*, **73**, 1067 (2001).
 [3] *Physics of traffic flow*, B. Kerner, Springer (2004).

[4] R. K une, A. Schadschneider, M. Schreckenberg and D.E. Wolf (eds.) *Traffic and Granular flow 05*, (Springer, 2007).
 [5] O. Biham, A. Middleton and D. Levine, *Phys. Rev. A*,

- 46, R6124 (1992).
- [6] T. Nagatani, *J. Phys. Soc. Japan*, **63**, 1228 (1994); *J. Phys. Soc. Japan*, **64**, 1421 (1995).
- [7] T. Nagatani, *Phys. Rev. E*, **51**, 922 (1995); and T. Seno, *Physica A*, **207**, 574 (1994).
- [8] J.A. Cuesta, F.C. Martines, J.M. Molera and A. Sanchez, *Phys. Rev. E*, **48**, R4175 (1993).
- [9] J. Freund and T. Pöschel, *Physica A*, **219**, 95 (1995).
- [10] B. Chopard, P.O. Luthi and P.A. Queloz *J. Phys. A*, **29**, 2325 (1996).
- [11] S. Tadaki, *Phys. Rev. E*, **54**, 2409 (1996); *J. Phys. Soc. Jpn.* **66**, 514 (1997).
- [12] J. Török and J. Kertesz, *Physica A*, **231**, 515 (1996).
- [13] H.F. Chau, K.Y. Wan and K.K. Yan, *Physica A*, **254**, 117 (1998).
- [14] D. Chowdhury and A. Schadschneider, *Phys. Rev. E*, **59**, R 1311 (1999).
- [15] E. Brockfeld, R. Barlovic, A. Schadschneider and M. Schreckenberg, *Phys. Rev. E*, **64**, 056132 (2001).
- [16] Y. Chiturr and B. Piccoli, *Discrete and Continuous Dynamical Systems B*, **5**, 599 (2005).
- [17] T. Nagatani, *J. Phys. A*, **26**, 6625 (1993).
- [18] Y. Ishibash and M. Fukui, *J. Phys. Soc. Japan*, **65**, 2793 (1996).
- [19] Y. Ishibash and M. Fukui, *J. Phys. Soc. Japan*, **70**, 2793 (2001); *J. Phys. Soc. Japan*, **70**, 3747 (2001).
- [20] M.E. Fouladvand and M. Nematollahi, *Eur. Phys. J. B*, **22**, 395 (2001).
- [21] M. Krbalek and P. Sebra, *J. Phys. A*, **36**, L7 (2003).
- [22] M. E. Fouladvand, Z. Sadjadi and M. R. Shaebani *J. Phys. A: Math. Gen.*, **37**, 561 (2004).
- [23] M. E. Fouladvand, Z. Sadjadi and M. R. Shaebani *Phys. Rev. E*, **70**, 046132 (2004).
- [24] M. E. Fouladvand, M. R. Shaebani and Z. Sadjadi *J. Phys. Soc. Japan*, **73**, No. 11, 3209 (2004).
- [25] D. Helbing, S. Lämmmer and J.P. Lebacque, in C. Deisenberg and R.F. Hartl(eds.), *Optimal Control and Dynamic Games*, p. 239, Springer, Dordrecht, 2005; arXiv physics/0511018.
- [26] S. Lämmmer, H. Kori, K. Peters and D. Helbing, *Physica A*, **363**, 39 (2006).
- [27] R. Jiang, D. Helbing, P. Kumar Shukla and Q-S Wu; *Physica A*, **368**, issue 2, 567 (2006).
- [28] B. Ray and S.N. Bhattacharyya, *Phys. Rev. E*, **73**, 036101 (2006).
- [29] R. X. Chen, K. Z. Bai and M. R. Liu, *Chinese Physics*, **15**, Issue 7, 1471 (2006).
- [30] R. Wang, M. Liu, R. Kemp and M. Zhou, *Int. J. Mod. Phys. C*, **18**, issue 5, 903 (2007).
- [31] D. W. Huang, *Physica A*, **383**, Issue 2, 603 (2007).
- [32] M. Najem, *Int. J. Mod. Phys. C*, **18**, Issue 6, 1047 (2007).
- [33] M. E. Fouladvand and S. Belbasi, *J. Phys. A: Math. Theor.*, **40**, 8289 (2007).
- [34] M. E. Fouladvand and M. Neek Amal, *Euro. Phys. Lett.*, **80**, issue 6, Article number 6002 (2007).
- [35] K. Nagel, M. Schreckenberg, *J.Phys. I France*, **2**, 2221 (1992).
- [36] G. M. Schütz, *J. Stat. Phys.*, **71**, 471 (1993).
- [37] H. Hinrichsen and S. Sandow *J. Phys. A: Math. Gen.*, **30**, 2745 (1997).
- [38] S. Janowsky and J. Lebowitz *Phys. Rev. A*, **45**, 618 (1992).
- [39] G. Tripathy and M. Barma, *Phys. Rev. Lett.*, **78**, 3039 (1997).
- [40] A. B. Kolomeisky, *J. Phys. A: Math. Gen.*, **31**, 1153 (1998).
- [41] K.H. Chung and P.M. Hui, *J. Phys. Soc. Jap.*, **63**, 4338 (1994).
- [42] S. Yukawa, M. Kikuchi and S. Tadaki *J. Phys. Soc. Jap.*, **63**, 3609 (1994).
- [43] B. Eisenblätter, L. Santen, A. Schadschneider and M. Schreckenberg, *Phys. Rev. E*, **57**, 1309 (1998).
- [44] F. Webster and B. Cobb in *Traffic Signal Setting*, (H.M.S Office, London, 1966).
- [45] M. G. Bell, *Transp. Res. A*, **26**, No.4, 303 (1992).